Ballistic spin filtering across ferromagnet/semiconductor interfaces at room temperature

A. Hirohata,* S. J. Steinmueller, W. S. Cho, Y. B. Xu,† C. M. Guertler, G. Wastlbauer, and J. A. C. Bland‡
Cavendish Laboratory, University of Cambridge, Madingley Road, Cambridge CB3 0HE, England

S. N. Holmes
Cambridge Research Laboratory, Toshiba Research Europe Limited, 260 Cambridge Science Park,
Milton Road, Cambridge CB4 0WE, England
(Received 9 February 2001; published 25 July 2002)

Circularly polarized light was used to generate spin-polarized electrons at room temperature in ferromagnet/GaAs Schottky diode structures (with spin polarization perpendicular to the film plane). The Schottky barrier dependence of the helicity-dependent photocurrent was observed using various ferromagnetic materials (NiFe, Co, and Fe) and GaAs doping densities. A change in the helicity-dependent photocurrent was obtained in all cases in reverse bias when the ferromagnetic layer magnetization was realigned from perpendicular to parallel to the photon helicity. This effect is attributed to spin filtering of photoexcited electrons generated in the GaAs due to the spin split density of states at the Fermi level in the ferromagnet which occurs when the magnetization is aligned with the photon helicity. NiFe shows significant spin filtering, Fe shows either strong or weak spin filtering according to the Schottky barrier strength, while Co shows almost none. Antiferromagnetic Cr/GaAs shows no spin-dependent effects as expected. These spin transport effects in all cases vanish for very high doping due to the collapse of the Schottky barrier. As the photon energy approaches the energy gap of the GaAs, the effects associated with the optically induced spin polarization in the GaAs become larger, confirming that polarized electrons are first excited in the semiconductor and then filtered by the ferromagnetic layer. The spin filtering effects in all cases increase with increasing ferromagnetic layer thickness, and are much larger than the estimated magnetocircular dichroism in permalloy. These results unambiguously indicate that highly efficient spin transport from the semiconductor to the ferromagnet occurs at room temperature and that strong spin filtering occurs in reverse bias.

DOI: 10.1103/PhysRevB.66.035330 PACS number(s): 75.25.+z, 73.30.+y, 73.61.−r, 78.66.−w

I. INTRODUCTION

Spin electronic devices based on the manipulation of spin-polarized electrons offer, in principle, the promise of significant advances in device performance, in terms of speed, size scaling, and power requirements.[1,2] Proposed spin analogues to conventional electronic devices have recently stimulated great interest, e.g., the spin-polarized field effect transistor (spin FET)[3,4] and the spin-polarized light-emitting diode (spin LED).[5,6] In order to realize such spin electronic devices, spin-dependent electron transport needs to be better understood. It is very important to note that efficient spin-dependent transport depends on achieving both efficient spin injection from a ferromagnet (FM) to a semiconductor (SC),[5–14] and efficient spin detection for electrons passing from the SC to the FM.[15] Efficient spin injection has been reported by Fiederling[5] and Ohno[6] using a magnetic SC but only at low temperature in all SC device structures. Spin injection has also been reported for a FM-metal/two-dimensional electron gas (2DEG) device at 75 K by Hammar *et al.*[7] Spin injection as well as detection has also been observed in similar structures up to 295 K.[8] Recently, spin injection from Fe into GaAs has been achieved successfully at room temperature with an efficiency of 2%[9] and 30%.[10] The question remains as to whether room-temperature efficient operation is possible and also whether strong spin transmission can be achieved between FM metals and SC. Theoretically, it has been suggested that there may be fundamental obstacles to achieving efficient spin transmission across FM-metal/SC interfaces via a diffusive electron transport process,[16] while it is expected that spin-dependent electron transport can be achieved at FM/SC interfaces with low transmission barriers.[17] On the other hand, very few studies have been conducted on spin detection and further clarification of the mechanisms involved is highly desirable.

One way of detecting spin-dependent electron transport is based on the use of photoexcitation techniques.[18] The possibility of passing a spin-dependent current through thin film tunnel junctions of both Co/Al_2O_3/GaAs and Co/τ-MnAl/AlAs/GaAs using photoexcited spin-polarized electrons has been discussed by Prins *et al.*[18] For the former structure, a spin-dependent tunneling current was reported, while only magneto-optical effects were seen in the latter structure. Accordingly a great many studies of spin-dependent tunneling through metal/oxide insulator/semiconductor (MOS) junctions have been reported.[19] As the photoexcitation measurements have been performed using back illumination of the circularly polarized light, optically excited electrons in the SC can be used to realize spin-polarized scanning tunneling microscopy (SP-STM) using sharp SC tips as theoretically proposed.[20,21] Some recent experiments suggest that such SP-STM may provide magnetic information.[22,23]

We previously found a significant spin filtering effect across FM/SC Schottky interfaces using photoexcitation techniques.[24] Recently Isakovic *et al.* have reported a similar effect,[25] however, they have focused on the influence of quantum wells in the SC on spin transport across the FM/SC interfaces. In this paper, we present the results of a system-

0163-1829/2002/66(3)/035330(11)/$20.00 ©2002 The American Physical Society

atic study of spin filtering as a function of FM material, FM layer thickness, GaAs doping density, and applied magnetic field. We also check possible magneto-optical effects in the SC by varying the applied magnetic field. Polarized photoexcitation in FM/SC structures was employed to create a population of spin-polarized electrons mainly in the SC substrate (GaAs). Their spin-dependent transport across the FM/SC interface at room temperature is detected as an electrical response, the strength of which varies according to the configuration of the photon helicity with respect to the magnetization in the FM layer. This setup is basically the reverse of that used for measurements of electroluminescence (EL) at the FM/SC interface by Alvarado *et al.*[26] and LaBella *et al.*,[27] for example. We achieved a change in helicity-dependent photocurrent when the magnetization was realigned from perpendicular to parallel to the helicity, which is attributed to spin filtering at the interface due to the spin splitting at the Fermi level in the FM. The Schottky barrier dependence of the helicity-dependent photocurrent was observed using various ferromagnetic materials and GaAs doping densities. NiFe shows significant spin filtering, Fe shows either strong or weak spin filtering according to the Schottky barrier strength, while Co shows almost no spin filtering. Antiferromagnetic (AF) Cr layers show no spin filtering as expected. These spin transport effects decrease with increasing doping density of the GaAs substrates but increase with increasing FM thickness and applied field. As the photon energy approaches the energy gap of the GaAs, the effects associated with the spin polarization in the GaAs substrate become larger, confirming that polarized electrons excited in the SC are filtered by the FM only when the magnetization is aligned with the photon helicity. From these results, the spin polarization is estimated and a simple model for the spin transport mechanism across the Schottky barrier is also discussed.

II. EXPERIMENTAL PROCEDURE

We used ultrahigh vacuum (UHV) deposition techniques to fabricate 5-nm-thick $Ni_{80}Fe_{20}$, Co, Fe, and Cr layers directly onto GaAs ($n=10^{23}$, 10^{24}, and $p=10^{25}$ m^{-3}) substrates, capped with 3-nm-thick Au layers. While Co and Fe can grow epitaxially on GaAs substrates,[24,28] polycrystalline samples were prepared here, however, NiFe does not grow epitaxially [the epitaxial relationship is Co(001)⟨110⟩‖GaAs(001)⟨110⟩ for Co/GaAs and Fe(001)⟨100⟩‖GaAs(001)⟨100⟩ for Fe/GaAs[29]]. A bias voltage was applied between one Au electrical contact on the surface of the sample and one ohmic contact attached to the back of the substrate. The current flowing through these two pads was measured (both with and without photoexcitation), while the voltage across the sample was also measured using a separate top contact as shown in Fig. 1.[24,28] The ohmic contacts on the bottom of the *n*- and *p*-type substrates were prepared by evaporating 100-nm-thick GeAuNi and AuBe respectively, and then annealed at 770 K for two minutes. The GaAs substrates were cleaned for two minutes using an oxygen plasma associated with chemical cleaning with acetone and isopropanol, and loaded into the UHV chamber.[24]

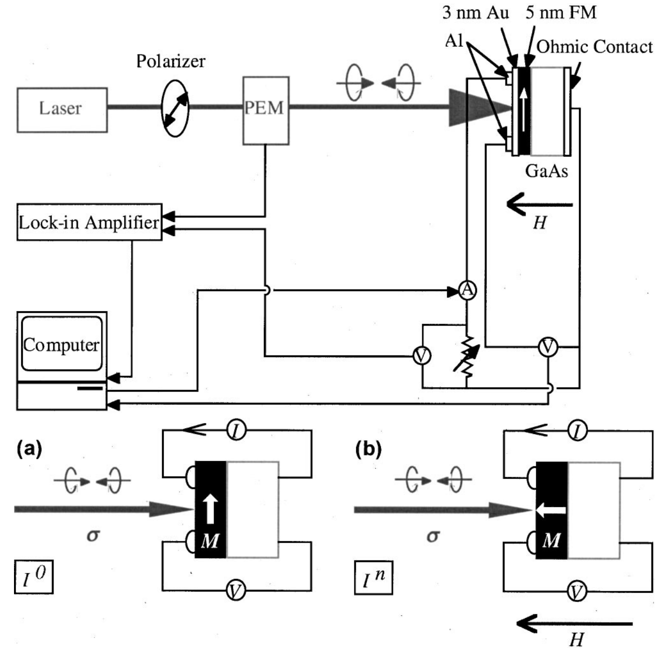

FIG. 1. Schematic configuration of the photoexcitation experiment. The laser ($h\nu=1.59$, 1.96, and 2.41 eV, and power 30, 5, and 3 mW, respectively) is polarized in the 45° direction. Right/left circular light is produced using a PEM. The bias dependent photocurrent is determined by I-V measurement methods combined with a lock-in technique. A schematic view of the FM/GaAs hybrid structure (3 mm×3 mm) is also shown in this diagram. Two Au contacts on the surface (0.5 mm×0.5 mm×550 mm) and an ohmic contact on the bottom are used for the measurement. The value of the variable resistance for the measurement was chosen to be approximately the same as that of the resistance between the FM and the GaAs substrate. The magnetization **M** in the FM and the photon helicity σ are shown with the field applied normal to the sample. Experimental configurations, (a) without (I^0) and (b) with (I^n) a magnetic field, are also shown in the inset.

The FM films were deposited at a rate of approximately one monolayer per minute by *e*-beam evaporation. The substrate temperature was held at 300 K and the pressure was around 7×10^{-10} mbar during growth. The deposition rate was monitored by a quartz microbalance calibrated by atomic force microscopy (AFM).

A circularly polarized laser beam (with the photon energy $h\nu$ in the range $1.59\leqslant h\nu\leqslant2.41$ eV) was used together with an external magnetic field to investigate the spin dependence of the photoexcited electron current at room temperature. The polarization of the beam was modulated from right to left circular using a photoelastic modulator (PEM) with 100% circular polarization at a frequency of 50 kHz. For the polarized illumination mode, the bias dependence of the ac helicity-dependent photocurrent I through the interface was probed both (a) in the remanent state (I^0) and (b) under the application of a magnetic field ($H=1.8$ T) sufficient to saturate the magnetization along the plane normal (I^n). As the polarized laser beam enters from the Au capping layer side, these structures provide a way of avoiding laser absorption at the bottom surface of the SC, as occurs under back illumination.[30]

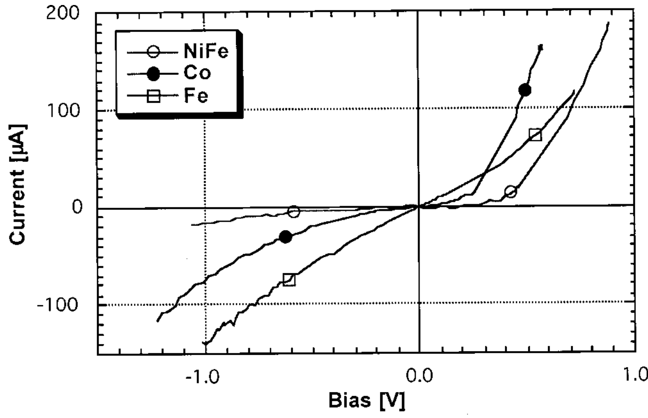

FIG. 2. Bias dependence of the current through the FM/GaAs (110) interface without photoexcitation (I-V curve) for the case of $Ni_{80}Fe_{20}$/GaAs ($n=10^{23}$ m^{-3}), Co/GaAs ($n=10^{24}$ m^{-3}), and Fe/GaAs ($n=10^{23}$ m^{-3}).

III. RESULTS AND DISCUSSIONS

A. Schottky characteristics with various ferromagnetic materials

Figure 2 shows the I-V curves of the FM/GaAs (110) samples measured without photoexcitation. Since the growth of the FM transition metals (Co and Fe) on GaAs substrates has been well established,[24] GaAs substrates were chosen for the present study.[30] The Schottky barrier (ϕ_b) of these samples varies as the barrier defines the shape of the I-V curves via the Shockley equation.[31]

The value of the ideality factor n[31] was found to be 4.85 and 9.5 for NiFe and Co, respectively ($n=1$ with the ideal Schottky barrier diode), while in the case of Fe, the I-V characteristic is often almost ohmic. In general, for Fe/GaAs samples, Schottky characteristics with a very small barrier height can be seen, but the barrier height strongly depends on the Fe/GaAs interface conditions (see the details in Sec. III D). It should be noted that the I-V curves of both NiFe and Co samples also contain ohmic linear components indicating that these samples behave as leaky Schottky diodes (this is partially due to the fact that we employed a three contact measurement rather than a true four contact geometry). However, in the parts of the sample which contribute to the diode-like behavior, tunneling across the Schottky barrier can be expected to occur and this is the dominant process in these samples for the I-V characteristic with $V<\phi_b$.

B. Helicity-dependent photocurrent with NiFe as the ferromagnet

1. SC doping density dependence

A key issue is the process (tunneling, thermionic emission, etc.) by which electrons are transported from the SC to the FM. The probability for tunneling is determined by the Schottky barrier height and depletion layer width. The depletion layer width W is defined by

$$W=\sqrt{\frac{2\varepsilon_S}{qN_D}(V_{bi}-V)}, \tag{1}$$

where N_D, ε_S, q, V_{bi}, and V stand for doping density, static dielectric constant, electron charge, built-in potential across the depletion layer, and applied bias, respectively. For GaAs, $\varepsilon_S=13.1\times\varepsilon_0$ ($\varepsilon_0=8.85418\times10^{-12}$ F/m) and $V_{bi}\approx0.8$ V. At zero bias, W is estimated to be in the range 3.4 nm ($N_D=10^{25}$ m^{-3}) to 34 nm ($N_D=10^{23}$ m^{-3}). These values are of the same order as those for Si, in which the electron tunneling is reported to be dominant with $N_D>10^{23}$ m^{-3}.[31] When W is large, the electron tunneling is reduced due to the wide tunnel barrier, while the tunneling does not occur for very small W because of tunnel barrier breakdown. As the electron tunneling process through the Schottky barrier is the dominant process in the case of Si ($N_D\geqslant10^{23}$ m^{-3}),[32] we assume the electron tunneling process is similarly dominant for the I-V characteristic in our GaAs samples. One can expect the maximum tunneling effects around $N_D\sim10^{24}$ m^{-3} as shown later in this section (Sec. III B 1). The ohmic part of the I-V characteristic, discussed above, is associated with diffusive transport which we assume to be spin independent.[16] This process occurs in parallel with tunneling processes and is likely to occur at local defects, indicating that the observed spin-polarized signals in helicity-dependent photocurrents are diluted by ohmic components. In n-type samples, the photocurrent is principally due to photoexcited holes, which propagate into the FM. However, a small fraction of the electrons, i.e., those within a few nm of the interface, can be expected to tunnel or be ballistically transported to the FM. All of these processes could in principle be sensitive to the spin-split density of states (DOS) in the FM layer. Our discussion of the spin-dependent transmission process will, however, focus just on the tunneling of electrons through the Schottky barrier[25] followed by ballistic transport in the FM. In this case it is clear that a significant spin dependence could arise, due to the large difference in spin dependent DOS at E_F.

The helicity-dependent photocurrent I was measured by modulating the photon helicity from right (σ^+) to left (σ^-). The two helicity values correspond to opposite spin angular momentum values of the incident photons and the helicity gives rise to opposite spin polarizations of electrons photoexcited in the GaAs.[33] The magnetization (**M**) in the FM is aligned perpendicular ($H=1.8$ T) or in plane ($H=0$) using an external field. For $\sigma\|\mathbf{M}$ (or antiparallel), the electrons in the FM and the SC share the same spin quantization axis, while for $\sigma\perp\mathbf{M}$, on the other hand, the two possible spin states created by the circularly polarized light are equivalent when projected along the magnetization direction in the FM (see Fig. 3). Consequently, in the remanent state ($\sigma\perp\mathbf{M}$), since the magnetization **M** is orthogonal to the photoexcited spin polarization, both up and down spin-polarized electrons in the SC can flow into the FM, opposing the electron current from the FM. At perpendicular saturation ($\sigma\|\mathbf{M}$), on the other hand, the up spin electron current from the SC is filtered due to the spin split density of states at the Fermi level E_F of the FM,[34–36] i.e., only minority spin electrons contribute to the transmitted current from the SC to the FM. This means that a greater net negative current now flows with $\sigma\|\mathbf{M}$ than that for $\sigma\perp\mathbf{M}$, since the current from the metal to the SC is largely independent of the magnetization configuration. Spin filtering is therefore turned on or off by controlling the rela-

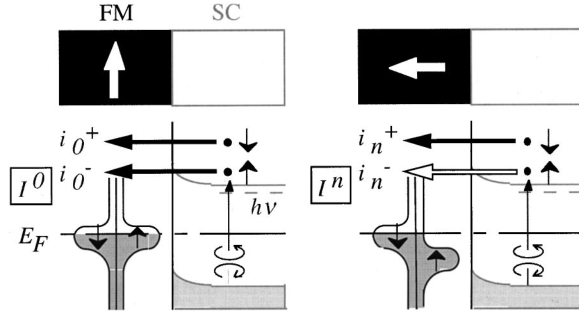

FIG. 3. Schematic diagrams illustrating the spin filtering mechanism for electron transport at the FM/SC interface. Averaged density of states of FM is shown for the case of I^0 for simplicity.

tive axes of σ and $\mathbf{M}$, and is detected as the helicity-dependent photocurrent I. With $\sigma \perp \mathbf{M}$, there is no spin filtering, while spin filtering is turned on by rotating to $\sigma \| \mathbf{M}$. The helicity-dependent photocurrents I^0 and I^n correspond to the magnetization configurations $\sigma \perp \mathbf{M}$ [see Fig. 1(a)] and $\sigma \| \mathbf{M}$ [see Fig. 1(b)], respectively. The helicity-dependent photocurrents I^0 and I^n are proportional to the difference between the current components for right (σ^+) and left (σ^-) circularly polarized light for each magnetization configuration: $I^0 = p^0 |i_0^+ - i_0^-|$ and $I^n = p^n |i_n^+ - i_n^-|$, where p^0 and p^n are phase factors for $\sigma \perp \mathbf{M}$ and $\sigma \| \mathbf{M}$, respectively. We shall discuss the measurement of the phase shift as a function of applied field later [see Sec. III B 3]. Since the autophase mode was used for the measurements of I^n and I^0, the phase factor was adjusted to be 1 in each case. As shown in Fig. 3, $i_0^+ = i_0^-$ is expected for the case of the remanent states, while $i_n^+ \neq i_n^-$ for the case of perpendicular saturation due to the spin polarization of the density of states at the Fermi level in the FM. In principle, the helicity-dependent photocurrent I^0 should be zero and I^n should reflect the electron spin polarization both in the SC and the FM.

The helicity-dependent photocurrent is shown in Fig. 4 with (I^n) and without (I^0) perpendicular saturation with various photon energies. In the case of $n = 10^{23}$ m^{-3} with $h\nu = 1.96$ eV [see Fig. 4(b)], for instance, the helicity-dependent photocurrent values for I^n and I^0 are observed to satisfy $|I^0| < |I^n|$ as expected. A phase shift between I^n and I^0 is also observed from the lock-in amplifier as expected but we observe that $|I^0| \neq 0$ in contrast to the prediction of the simple model (see the detailed discussion in Sec. III B 3). The offset in $|I^0|$ is not an experimental artifact as evidenced by the fact that it is not observed in Fe and Co samples (see Secs. III C and III D, respectively). The difference between I^n and I^0 provides clear evidence that spin-dependent transport from the SC to the FM occurs under the application of a perpendicular magnetic field. It should be emphasized that the values of I^0 are unique to the samples. The fact that $|I^0| \neq 0$ is likely to be a consequence of the simplified nature of our spin filtering model, which ignores, for example, spin-polarized electrons excited in the FM which propagate to the SC and hole transport from the SC to the FM. The bias dependence of the helicity-dependent photocurrent difference $\Delta I (= I^n - I^0)$ of ~ 0.015 μA is almost constant in the bias range of $V < 0.7$ V. Comparing the magnitude of the

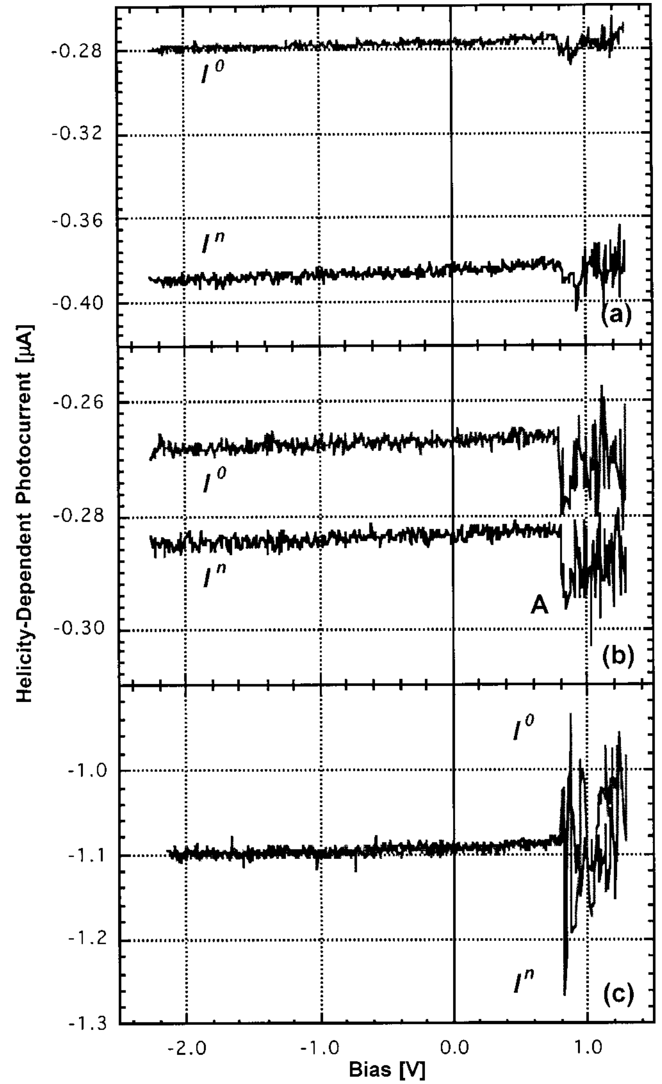

FIG. 4. Bias dependence of the helicity-dependent photocurrent without (I^0) and with the applied magnetic field (I^n) for the case of NiFe/GaAs ($n = 10^{23}$ m^{-3}) induced by a photon energy of $h\nu$ = (a) 1.59, (b) 1.96, and (c) 2.41 eV.

photocurrent obtained with unpolarized light (approximately a few mA), ΔI is two orders of magnitude smaller than the photocurrent.

To test the role of the Schottky barrier, we investigated samples with various doping densities of the GaAs. Figure 5(a) shows the I-V curves of the $Ni_{80}Fe_{20}$ samples with various GaAs doping densities obtained without photoexcitation measured by the usual method at room temperature employing separate current and voltage contacts (a common connection is used at the back of the substrates). Every I-V curve possesses a small feature (A) around the Schottky barrier height, which corresponds to a feature A in Fig. 4(b), as observed previously.[28] The ideality factor was calculated to be 6.69, 5.37, and 4.04 for $n = 10^{23}$, 10^{24}, and $p = 10^{25}$ m^{-3}, respectively. These samples also contain weak ohmic components, which give rise to a degree of linearity in the I-V curves around zero bias. As the doping density increases, the Schottky barrier height ϕ_b is observed to de-

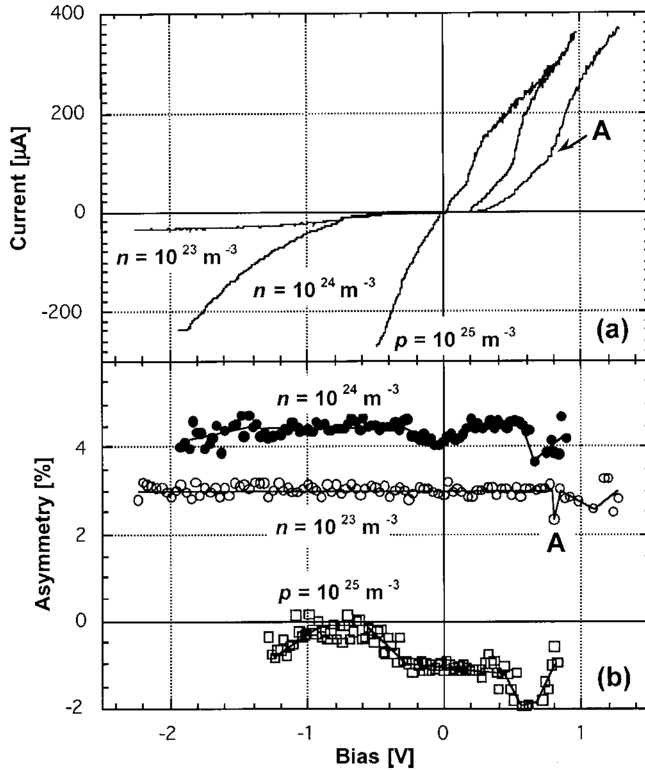

FIG. 5. (a) Bias dependence of current through the $Ni_{80}Fe_{20}/GaAs$ ($n=10^{23}$, 10^{24}, and $p=10^{25}$ m^{-3}) interface obtained without photoexcitation (I-V curve). (b) Bias dependence of asymmetry $A=(I^n-I^0)/(I^n+I^0)$ with $Ni_{80}Fe_{20}/GaAs$ ($n=10^{23}$, 10^{24}, and $p=10^{25}$ m^{-3}).

crease from approximately 0.8 ($n=10^{23}$ m^{-3}) to 0.2 eV ($p=10^{25}$ m^{-3}) in the NiFe/GaAs hybrid structures as expected.[28]

The asymmetry of the spin-polarized current through the NiFe/GaAs interface $A=(I^n-I^0)/(I^n+I^0)$ induced by He-Ne laser light ($h\nu=1.96$ eV) is shown in Fig. 5(b) for three different values of the GaAs doping density. With $n=10^{24}$ m^{-3}, for example, an almost constant asymmetry ($A\sim4.5\%$) can be seen in the bias range of $-1.5<V<0.3$ V, which we attribute to the spin-polarized photocurrent propagating from the SC to the FM as discussed above. For $n=10^{23}$ m^{-3}, the corresponding value is $A\sim3\%$, while for $p=10^{25}$ m^{-3}, $A\sim0$. It should be noted that these values of A depend on the resistivity across the FM/SC interface. The total resistance is 60, 200, and 15 Ω for the $n=10^{23}$, 10^{24}, and $p=10^{25}$ m^{-3} doped substrates, respectively. We conclude from the above results that the magnitude of the spin-polarized current in reverse bias scales with the Schottky barrier height, as is expected for spin-polarized tunneling across the barrier. For sufficiently large doping, the Schottky barrier is suppressed.

Since the spin coherence length has been reported to decrease with the SC doping density,[31,37] the spin filtering effect is expected to be reduced at very high doping density. Both the tunneling barrier and the spin coherence length play a key role in our helicity-dependent photoexcitation measurements as seen in Fig. 5(b). We note that spin injection processes[38] may also occur according to the applied bias.

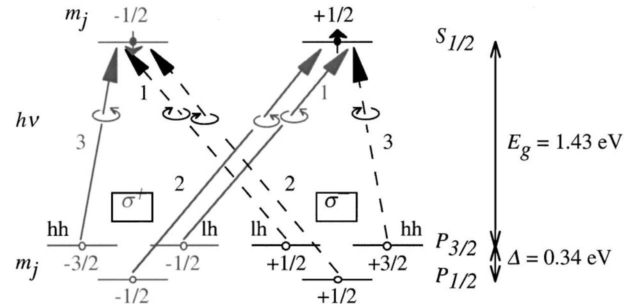

FIG. 6. Schematic diagram of the allowed transitions for right (σ^+, solid lines) and left (σ^-, dashed lines) circularly polarized light with GaAs at room temperature. The selection rule is $\Delta m_j=+1$ for σ^+ and $\Delta m_j=-1$ for σ^-. The numbers near the arrows represent the relative transition probabilities. The magnetic quantum numbers are also indicated at the energy levels. The heavy and light holes are abbreviated to *hh* and *lh*, respectively.

2. Photon energy dependence

The helicity-dependent photocurrent curves shown in Fig. 4 for the $n=10^{23}$ m^{-3} doped sample correspond to the photon energy range $1.59\leq h\nu\leq2.41$ eV. With $h\nu=1.59$ eV, for example, an almost constant difference between the helicity-dependent photocurrent for the two configurations ($\Delta I=I^n-I^0$) is again seen at negative bias [see Fig. 4(a)]. Minor increases in both I^0 and I^n are obtained with increasing bias which resemble the form of the usual I-V characteristic seen without photoexcitation. It should be emphasized that the helicity-dependent photocurrent values for perpendicular (I^0) and parallel (I^n) configurations are always observed to satisfy $|I^0|<I^n|$. This observation provides clear evidence that spin-polarized filtering of polarized electrons generated in the SC occurs in the FM under the application of a perpendicular magnetic field. It should also be noted that the helicity-dependent current difference ΔI decreases from -110 nA to zero with increasing photon energy.

In GaAs, the valence band maximum and the conduction band minimum are at Γ with an energy gap $E_g=1.43$ eV at room temperature, indicating that the only transitions induced by the photon energy $h\nu$ occur at Γ (direct gap semiconductor).[33,39] The valence band (p-symmetry) splits into fourfold degenerate $P_{3/2}$ and twofold degenerate $P_{1/2}$ states, which lie Δ=0.34 eV below $P_{3/2}$ at Γ, whereas the conduction band (s symmetry) is twofold degenerate $S_{1/2}$ as schematically shown in Fig. 6. When $h\nu=E_g$, circularly polarized light excites electrons from $P_{3/2}$ to $S_{1/2}$. According to the selection rule ($\Delta m_j=\pm1$), the two transitions for each photon helicity (σ^+ and σ^-) are possible, however the relative transition probabilities for light and heavy holes need to be taken into account in order to estimate the net spin polarization.[33] Although the maximum polarization is expected to be 50% in theory, the maximum is experimentally observed to be ~40% at the threshold.[5,33] For $E_g+\Delta<h\nu$, the polarization decreases due to the mixture of light and

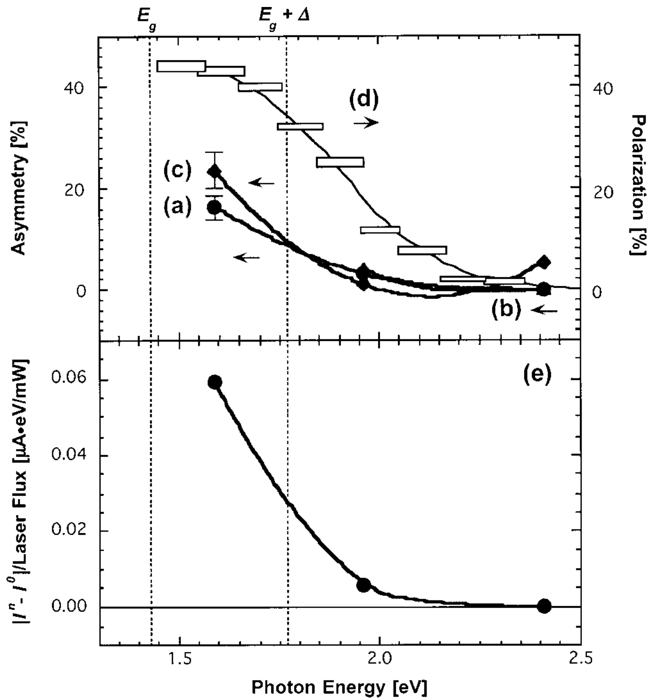

FIG. 7. Photon energy dependence of asymmetry at $V=0$ V for the case of $Ni_{80}Fe_{20}$/GaAs [(a) $n=10^{23}$, (b) 10^{24}, and (c) $p=10^{25}$ m^{-3}]. For the $p=10^{25}$ m^{-3} sample, the absolute value of asymmetry A is shown in the figure. (d) Spin polarization in GaAs measured by photoemission experiment is also shown in Ref. 33. Photon energy dependence of $|\Delta I|$/laser flux is also shown in (e).

heavy hole states with the split-off valence band states, which have an opposite sign.[33]

We expect that the asymmetry A should fall with increasing photon energy in our experiments, thus providing a crucial test of the proposed spin filtering mechanism. Figure 7 shows that the asymmetry A at zero bias decreases with increasing induced photon energy in the range $1.59 \leqslant h\nu \leqslant 2.41$ eV. The spin polarization curve for GaAs obtained by photoemission is also shown for Ref. 33. A clear trend is observed with increasing A as the photon energy approaches E_g. For the $n=10^{23}$ m^{-3} doped sample, for instance, A decreases from 16% ($h\nu=1.59$ eV) to zero ($h\nu=2.41$ eV) with increasing photon energy, which indicates that the spin polarization vanishes at high photon energy as expected. The $n=10^{24}$ m^{-3} sample shows a similar photon energy dependence of the asymmetry A. It is important to note that such a photon energy dependence is opposite from the photon energy dependence of the expected magnetic circular dichroism (MCD) effects in FM NiFe, which decrease with decreasing photon energy.[40] It should also be noted that the $p=10^{25}$ m^{-3} sample provides negative values for A (due to the different shape of the Schottky barrier compared with that of the n-type doped samples) which again confirm the photon energy dependence.

We also show the photon energy dependence of $\Delta I/P$ [P: photon flux (=laser power/photon energy)], which is proportional to the electron spin polarization, in Fig. 7(e). It should be emphasized that this result shows a similar photon energy dependence as does the asymmetry A, supporting our model of spin filtering effects, in which the spin polarization of the photoexcited electrons is determined by the photon energy.

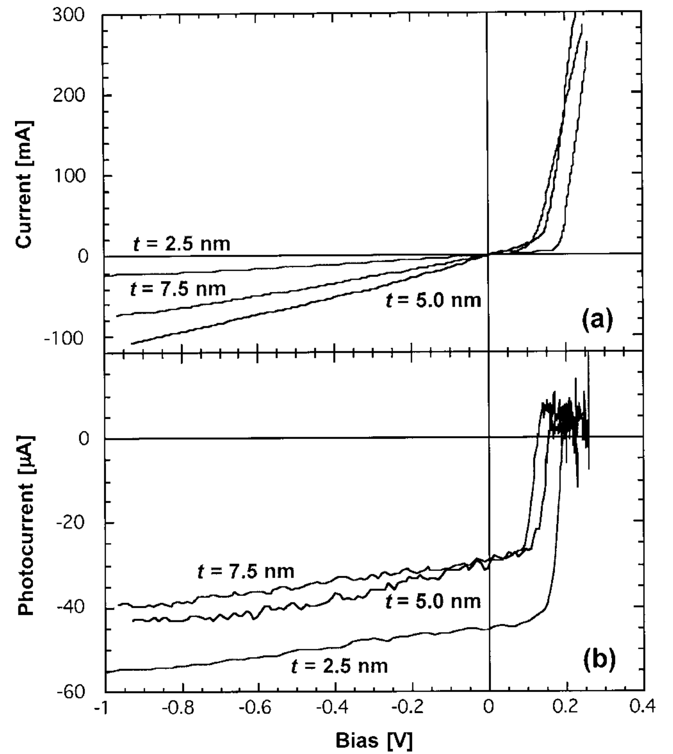

FIG. 8. Bias dependence of the (a) dc current and (b) photocurrent obtained with unpolarized photoexcitation through the t-nm thick ($t=2.5$, 5.0, and 7.5 nm) NiFe/GaAs (100) ($n=10^{23}$ m^{-3}).

3. FM layer thickness dependence

Figure 8(a) shows the I-V curves of NiFe samples prepared with three different thicknesses ($t=2.5$, 5.0, and 7.5 nm) measured in the same way as described above. All the curves show Schottky characteristics as described in Secs. III A and III B 1, and are similar to the 5-nm-thick permalloy samples discussed in Sec. III B 1. The bias dependence of the unpolarized photocurrent is shown in Fig. 8(b). The entire I-V curves are shifted to negative current values as expected for conventional Schottky diodes since minority carriers (holes) dominate the transport.[41] It should be noted that the unpolarized photocurrent approaches zero at $V \sim \phi_b$.

The bias dependences of the helicity-dependent photocurrent for the three permalloy samples are presented in Fig. 9. As before the helicity-dependent photocurrent is almost two orders of magnitude smaller than the unpolarized photocurrent as anticipated from our model but the bias dependence follows that of the unpolarized photocurrent. An almost constant difference between I^n and I^0 occurs as in the 5-nm samples discussed in Sec. III B 1. This indicates that although the bias dependence of both I-V and unpolarized photocurrent curves are dependent upon the specific interface characteristics of the samples, the helicity-dependent photocurrent curves are similar for all the NiFe samples. This find-

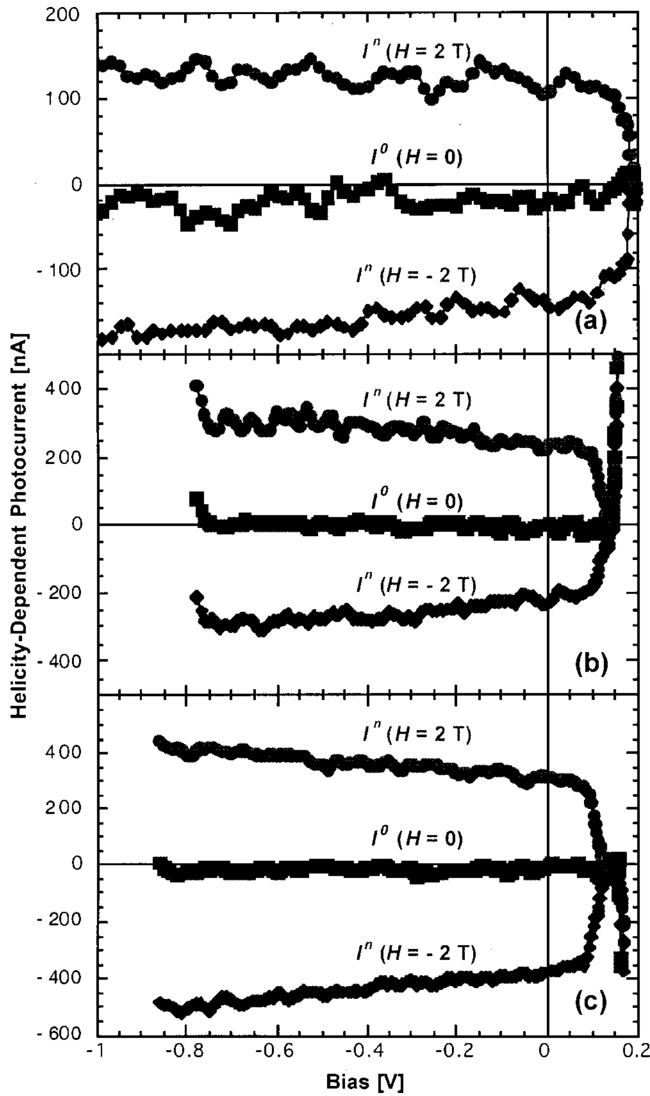

FIG. 9. Bias dependence of the helicity-dependent photocurrent without (solid line with closed squares I^0) and with the applied magnetic field of 2 T (solid line with closed circles and closed rhombuses I^n) in the case of NiFe/GaAs (100) ($n=10^{23}$ m^{-3}) with $t=$(a) 2.5, (b) 5.0, and (c) 7.5 nm.

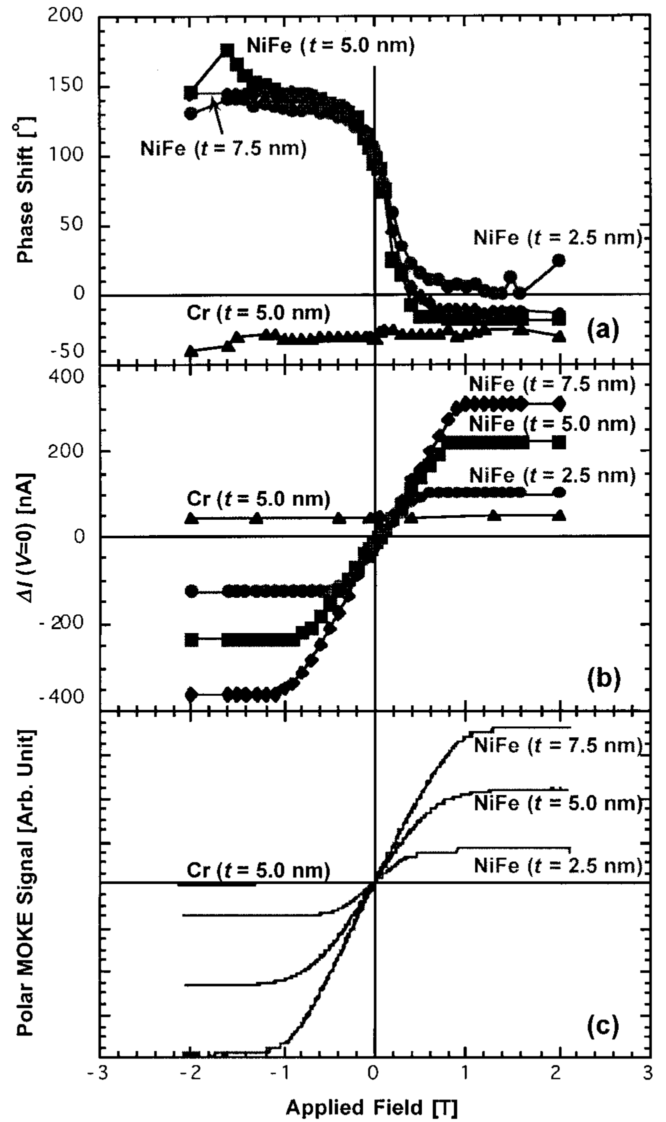

FIG. 10. Applied magnetic field dependence of (a) phase shift, (b) ΔI, and (c) MOKE signal for NiFe/GaAs (100) ($n=10^{23}$ m^{-3}) ($t=2.5$, 5.0, and 7.5 nm) and Cr/GaAs (100) ($n=10^{23}$ m^{-3}) samples.

ing again provides clear evidence of the existence of spin filtering effects at the FM/SC interface.

These samples show a very small offset in I^0 ($\sim$2.5 nA) and symmetric values between I^n ($H=2$ T) and I^n ($H=-2$ T). It should be emphasized that the difference $\Delta I=I^n-I^0$ increases with increasing the NiFe layer thickness t. In order to investigate the FM layer thickness dependence further and to explicitly exclude possible magneto-optical effects in the SC, we measured the applied magnetic field dependence of the spin filtering effect (see Fig. 10). First, the phase shift of the lock-in amplifier is measured and shows almost 180° change upon reversing the saturation magnetization direction in the NiFe samples as presented in Fig. 10(a). This indicates unambiguously that the magnetization alignment of the FM layer with respect to the photon helicity σ controls the spin filtering effect as expected from the discussion in Sec. III B 1. The results for antiferromagnetic (AF) Cr/GaAs are also shown in Fig. 10(a) for reference, which also confirms that the signals we observed are of FM layer origin. The details of AF Cr/GaAs samples are discussed in Sec. III E.

Similarly, the applied field dependence of ΔI without bias is shown in Fig. 10(b) for each thickness. Again, this figure clearly indicates that the spin filtering effect increases with t. Most importantly, the field dependence of ΔI matches that of the polar magneto-optical Kerr effect (MOKE) signals [see Fig. 10(c)], suggesting that there are no significant background effects due to Zeeman splitting in the GaAs.[9,25] Although the Cr samples show a small offset, they do not possess any field dependence (due to a possible SC-related background) as seen in Fig. 10(b), confirming that the Zeeman splitting effect is negligible in our measurement.

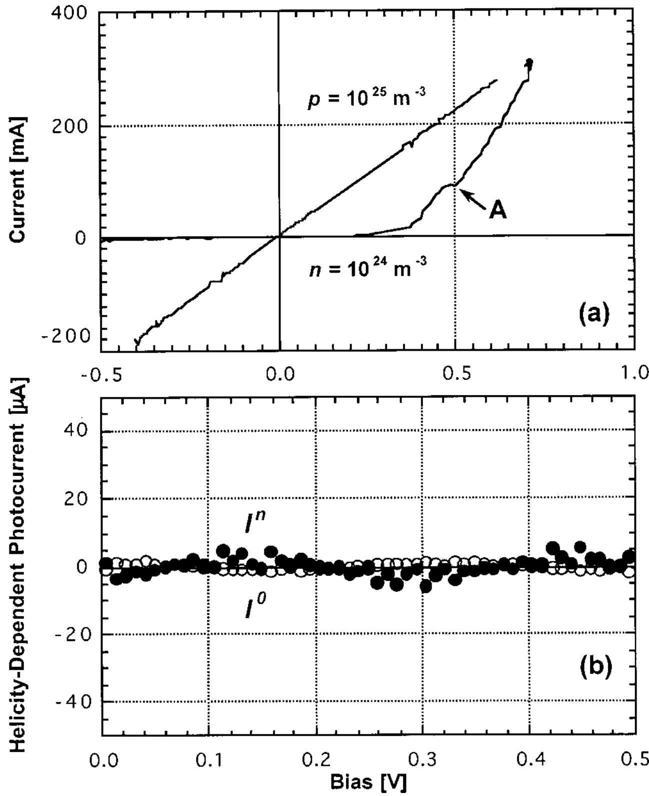

FIG. 11. (a) Bias dependence of current through the Co/GaAs (100) ($n = 10^{24}$ and $p = 10^{25}$ m^{-3}) interface obtained without photon excitation (I-V curve). Bias dependence of the helicity-dependent photocurrent without (open circles, I^0) and with the applied magnetic field (closed circles, I^n) with Co/GaAs (100) in the case of the doping density of (b) $n = 10^{24}$ m^{-3}.

C. Co as the ferromagnet

Figure 11(a) shows the I-V curves of the 5-nm-thick Co samples without photoexcitation. These curves clearly indicate that the Schottky barrier height ϕ_b falls with increasing doping density. It should be noted that the I-V curve with $n = 10^{24}$ m^{-3} possesses a small feature (A) at around the Schottky barrier height ϕ_b as observed with NiFe samples.

The helicity-dependent photocurrent is shown in Fig. 11(b) with (I^n) and without (I^0) perpendicular saturation for the value of doping $n = 10^{24}$ m^{-3}. I^0 is almost constant (~ -0.16 μA), while I^n is -0.20 ± 5.6 μA, i.e., large fluctuations occur. It should be noted that the photocurrent with unpolarized light is about -2.0 μA. These large fluctuations in I^n make an estimation of the difference $\Delta I = I^n - I^0$ difficult. The small value of ΔI observed suggests that the spin filtering in the Co/GaAs structure is much weaker than that in NiFe/GaAs in most of the bias range. With $p = 10^{25}$ m^{-3} (not shown), ΔI is approximately -35 nA, which is smaller than that with $n = 10^{24}$ m^{-3} and corresponds to a decrease with increasing doping density. Our simple spin transport model does not explain the difference between the Co and permalloy samples.

The asymmetry A decreases with increasing doping density as observed with the NiFe samples. The difference ΔI in the helicity-dependent photocurrents is also almost constant

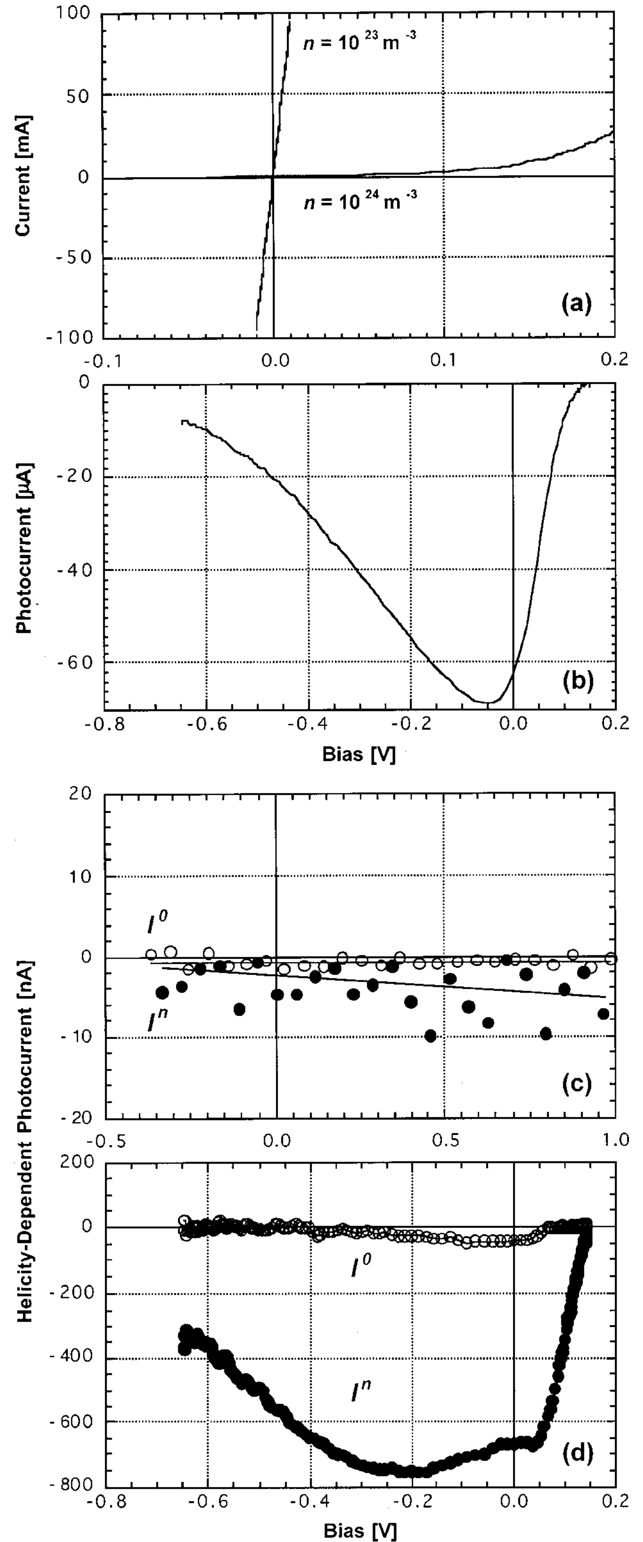

FIG. 12. (a) Bias dependence of current through the Fe/GaAs (100) ($n = 10^{23}$ and $n = 10^{24}$ m^{-3}) interface obtained without photon excitation (I-V curve). (b) Bias dependence of photocurrent with unpolarized photoexcitation with Fe/GaAs (100) ($n = 10^{24}$ m^{-3}). Bias dependence of the helicity-dependent photocurrent without (open circles, I^0) and with the applied magnetic field (closed circles, I^n) with Fe/GaAs (100) in the case of the doping density of (c) $n = 10^{23}$ and (d) 10^{24} m^{-3}.

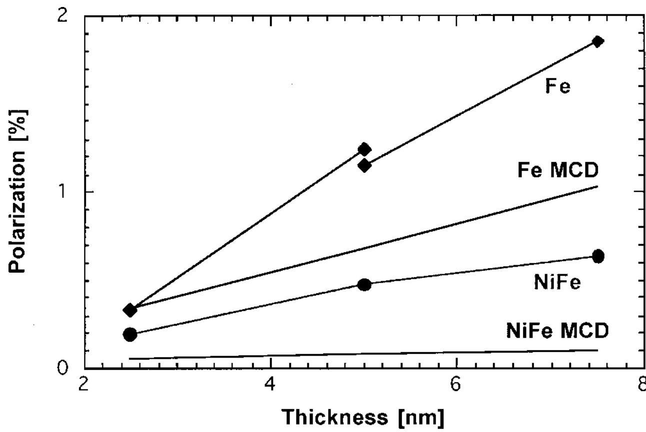

FIG. 13. Thickness dependence of spin polarization across the FM/GaAs interfaces for the case of both NiFe and Fe as the FM. The magnitude of the calculated MCD effects is also shown as positive values.

and is different from that observed with the Co/Al_2O_3/GaAs system, in which $\Delta I/I$ is of the order of a few % at reverse bias, diverges gradually at zero bias and does not show any peak at forward bias.[18,19] The spin filtering is therefore found to be very weak in the Co/GaAs structures for most of the bias range.[18] As MCD in Co has been reported to be ~0.15%,[19] the MCD effects could be important around zero bias.

D. Fe as the ferromagnet

Figure 12(a) shows the I-V curves of the 5-nm-thick Fe samples. Depending on the specific substrates used, very different I-V characteristics were observed. The curve with $n = 10^{23}$ m^{-3} is ohmic, while that with $n=10^{24}$ m^{-3} possesses a very weak Schottky barrier, but surprisingly, a lower impedance, again, probably due to the presence of defects.

The bias dependence of the helicity-dependent photocurrent for the case of $n=10^{23}$ m^{-3} is shown in Fig. 12(c). I^0 is almost constant (-0.92 nA), while I^n is approximately -4.3 nA). ΔI is again small and calculated to be about -3.4 nA. Since the photocurrent with unpolarized light is about -15 μA, the effects from the helicity-dependent photocurrent are clearly very small. No significant peak related to the Schottky barrier is seen, which is consistent with the ohmic characteristics of the Fe/GaAs samples. This result also provides a check on possible experimental asymmetries. The helicity-dependent photocurrent with $n=10^{24}$ m^{-3}, on the other hand, displays a clear difference between I^n and I^0 related to the presence of the significant Schottky barrier at the Fe/GaAs interface in this sample [see Fig. 12(d)]. It should be emphasized that the bias dependence of the photocurrent with unpolarized photoexcitation possesses a large peak around zero bias as shown in Fig. 12(b). These results clearly indicate that the presence of the Schottky barrier plays the crucial role in determining spin transport in FM/SC hybrid structures. The bias dependence of the helicity-dependent photocurrent for Fe samples is again different from permalloy and Co samples.

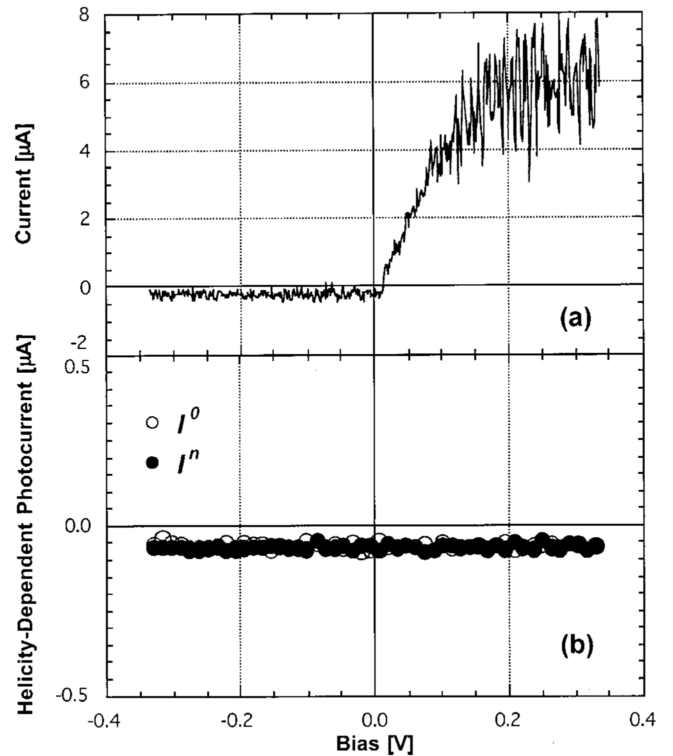

FIG. 14. (a) Bias dependence of current through the Cr/GaAs ($n=10^{23}$ m^{-3}) interface obtained without photon excitation (I-V curve). (b) Bias dependence of the helicity-dependent photocurrent without (open circles, I^0) and with the applied magnetic field (closed circles, I^n) with Cr/GaAs.

In order to study spin filtering effects quantitatively, we performed dc photoexcitation measurements. Circularly polarized light was generated using a λ/4 plate, and the dc helicity-dependent photocurrent was observed for both right (I^+) and left circular (I^-) configurations. The spin polarization of the spin filtering effects was estimated as $S=(I^+-I^-)/(I^++I^-)$. Figure 13 shows the thickness dependence of both the estimated spin polarization and the magnitude of the MCD effects for both NiFe and Fe. The spin polarization increases with the FM layer thickness t and is larger than calculated MCD effects as shown in Fig. 13. In particular, the spin polarization for the Fe samples approaches $2\pm1\%$ for the thickest sample (allowing for MCD effects), which is reasonably consistent with the spin injection efficiency of 2% in Fe/GaAs structures observed by Zhu *et al.*[9] at room temperature. A similar thickness dependence of spin polarization has been reported by Van't Erve *et al.*,[42] suggesting that spin filtering occurs in the ballistic regime. It should be noted that the signs of spin polarization for spin filtering are the same for both NiFe and Fe but the sign of the MCD is expected to be opposite for NiFe and Fe.[43]

E. Antiferromagnetic Cr as the metal layer

Figure 14(a) shows the I-V curve of a Cr sample without photoexcitation, which indicates that the sample behaves as a very good Schottky diode (the Schottky barrier height ϕ_b is very small and the ideality factor $n=1.53$) with a small off-

set in reverse bias. Since all the samples, including NiFe/GaAs, Fe/GaAs, Co/GaAs, and Cr/GaAs, are prepared using the same procedures, the combined results for these samples suggest that for some metals UHV deposition may not necessarily provide good Schottky characteristics.

The helicity-dependent photocurrent for the Cr/GaAs sample is shown in Fig. 14(b) with (I^n) and without (I^0) perpendicular saturation. There is no difference between I^n and I^0, suggesting that no spin-polarized electron current flows across the AF Cr/GaAs interface, as expected. This is one of the crucial tests for the validity of this photoexcitation study. The origin of the small offset in Cr/GaAs and NiFe/GaAs will be discussed elsewhere.[44]

IV. SUMMARY AND CONCLUSIONS

The Schottky barrier dependence of spin-polarized electron transport across FM/SC hybrid structures has been investigated using various ferromagnetic materials (NiFe, Co, and Fe) and GaAs doping densities. At room temperature, we observed a clear difference in the helicity-dependent photocurrent through the FM/GaAs interface according to the orientation of the sample magnetization with respect to the helicity. An almost constant and large difference between the helicity-dependent photocurrent for the two magnetization configurations is observed in reverse bias in permalloy but a bias dependence is seen for Fe samples with a Schottky barrier. In our simplified model this difference in photocurrent corresponds to a measure of the spin-polarized photocurrent tunneling from the SC to the FM and varies with doping density. Fe/GaAs also shows either strong or weak spin filtering (according to the Schottky characteristics), and we observe a maximum spin polarization of approximately 2%, which is consistent with the spin injection efficiency of 2% in Fe/GaAs structures observed by Zhu *et al.*;[9] on the other hand, Co/GaAs shows almost no spin filtering. AF Cr/GaAs shows no spin dependence as expected and provides an important test of the validity of our experiments. The helicity-dependent photocurrent asymmetry increases when the photon energy approaches the energy gap of the GaAs, confirming that spin-polarized electrons are first generated in the GaAs followed by spin filtering in the FM. The spin polarization also increases with the FM layer thickness, which provides further support of the view that spin filtering is associated with *ballistic transport in the metal*. These results unambiguously indicate that spin-polarized electrons are transmitted from the SC to the FM with high efficiency.

ACKNOWLEDGMENTS

We are grateful to Professor Guangxu Chen for the assistance with the Ar laser operation and Ken Cooper for his help with sample fabrication. The support of EPSRC, EU (Esprit program) and ETRI (Korea) is also acknowledged. A.H. would like to thank the Toshiba Europe Research Limited and the Cambridge Overseas Trust for their financial support. S.J.S. gratefully acknowledges the financial support of ABB (Sweden). W.S.C. was supported by the Korea Science & Engineering Foundation (KOSEF). G.W. would like to thank the Austrian Academy of Sciences and the Wilhelm-Macke-Stipendienprivatstiftung (Austria) for their financial support.

*Present address: Francis Bitter Magnet Laboratory, Massachusetts Institute of Technology, Cambridge, Massachusetts 02139.

†Present address: Department of Electronics, University of York, Heslington, York YO10 5DD, England.

‡Author to whom correspondence should be addressed. E-mail address: jacb1@phy.cam.ac.uk

[1] G. A. Prinz, Science **282**, 1660 (1998).

[2] M. Johnson, IEEE Spectrum **37**, 33 (2000).

[3] S. Datta and B. Das, Appl. Phys. Lett. **56**, 665 (1990).

[4] M. Johnson, Phys. Rev. B **58**, 9635 (1998).

[5] R. Fiederling, M. Keim, G. Reuscher, W. Ossau, G. Schmidt, A. Waag, and L. W. Molenkamp, Nature (London) **402**, 787 (1999).

[6] Y. Ohno, D. K. Young, B. Beschoten, F. Matsukura, H. Ohno, and D. D. Awschalom, Nature (London) **402**, 790 (1999).

[7] P. R. Hammar, B. R. Bennet, M. J. Yang, and M. Johnson, Phys. Rev. Lett. **83**, 203 (1999).

[8] P. R. Hammar and M. Johnson, Phys. Rev. B **61**, 7207 (2000).

[9] H. J. Zhu, M. Ramsteiner, H. Kostial, M. Wassermeier, H.-P. Schönher, and K. H. Ploog, Phys. Rev. Lett. **87**, 016 601 (2001).

[10] A. T. Hanbicki, B. T. Jonker, G. Itskos, G. Kioseoglou, and A. Petrou, Appl. Phys. Lett. **80**, 1240 (2002).

[11] A. Fert and S. F. Lee, J. Magn. Magn. Mater. **165**, 115 (1997).

[12] S. Gardelis, C. G. Smith, C. H. W. Barnes, E. H. Linfield, and D. A. Ritche, Phys. Rev. B **60**, 7764 (1999).

[13] M. Oestreich, J. Hübner, D. Hägele, P. J. Klar, W. Heimbrodt, W. W. Rühle, D. E. Ashenford, and B. Lunn, Appl. Phys. Lett. **74**, 1251 (1999).

[14] I. Malajovich, J. M. Kikkawa, D. D. Awschalom, J. J. Berry, and N. Samarth, Phys. Rev. Lett. **84**, 1015 (2000).

[15] S. K. Upadhyay, R. N. Louie, and R. A. Buhrman, Appl. Phys. Lett. **74**, 3881 (1999).

[16] G. Schmidt, D. Ferrand, L. W. Molenkamp, A. T. Filip, and B. J. van Wees, Phys. Rev. B **62**, R4790 (2000).

[17] E. I. Rashba, Phys. Rev. B **62**, R16 267 (2000).

[18] M. W. J. Prins, H. van Kempen, H. van Leuken, R. A. de Groot, W. van Roy, and J. de Boeck, J. Phys.: Condens. Matter **7**, 9447 (1995).

[19] K. Nakajima, S. N. Okuno, and K. Inomata, Jpn. J. Appl. Phys., Part 2 **37**, L919 (1998).

[20] S. N. Molotkov, Surf. Sci. **287/288**, 1098 (1993).

[21] R. Laiho and H. J. Reittu, Surf. Sci. **289**, 363 (1993).

[22] K. Sueoka, K. Mukasa, and K. Hayakawa, Jpn. J. Appl. Phys. **32**, 2989 (1993).

[23] Y. Suzuki, W. Nabhan, and K. Tanaka, Appl. Phys. Lett. **71**, 3153 (1997).

[24] A. Hirohata, Y. B. Xu, C. M. Guertler, J. A. C. Bland, and S. N. Holmes, Phys. Rev. B **63**, 104425 (2001).

[25] A. F. Isakovic, D. M. Carr, J. Strand, B. D. Schultz, C. J. Palmstrøm, and P. A. Crowell, Phys. Rev. B **64**, 161304 (2001).

[26] S. F. Alvarado and P. Renaud, Phys. Rev. Lett. **68**, 1387 (1992).

[27] V. P. LaBella, D. W. Bullock, Z. Ding, C. Emery, A. Venkatesan, W. F. Oliver, G. J. Salamo, P. M. Thibado, and M. Mortazavi, Science **292**, 1518 (2001).

[28] J. A. C. Bland, A. Hirohata, Y. B. Xu, C. M. Guertler, and S. N. Holmes, IEEE Trans. Magn. **36**, 2827 (2000).

[29] Y. B. Xu, E. T. M. Kermohan, D. J. Freeland, A. Ercole, M. Tselpi, and J. A. C. Bland, Phys. Rev. B **58**, 890 (1998).

[30] J. M. Kikkawa and D. D. Awschalom, Phys. Rev. Lett. **80**, 4313 (1998).

[31] S. M. Sze, *Physics of Semiconductor Devices* (Wiley, New York, 1981), pp. 245.

[32] Contacts to Semiconductors Fundamentals and Technology, edited by L. J. Brillson (Noyes Publications, New York, 1993), pp. 176.

[33] D. T. Pierce and F. Meier, Phys. Rev. B **13**, 5484 (1976).

[34] I. I. Mazin, Phys. Rev. Lett. **83**, 1427 (1999).

[35] B. Nadgorny, R. J. Soulen, Jr., M. S. Osofsky, I. I. Mazin, G. Laprade, R. J. M. van de Veerdonk, A. A. Smits, S. F. Cheng, E. F. Skelton, and S. B. Qadri, Phys. Rev. B **61**, R3788 (2000).

[36] C. Li, A. J. Freeman, and C. L. Fu, J. Magn. Magn. Mater. **75**, 53 (1988).

[37] J. M. Kikkawa, I. P. Smorchkova, N. Samarth, and D. D. Awschalom, Science **277**, 1284 (1997).

[38] A. Hirohata, Y. B. Xu, C. M. Guertler, J. A. C. Bland, and S. N. Holmes, in *Magnetic Materials, Structures and Processing for Information Storage*, edited by B. J. Daniels *et al.*, Mater. Res. Soc. Symp. Proc. No. **614** (Materials Research Society, Warrendale, 2001), p. F5.4.

[39] S. Adachi, *GaAs and Related Materials* (World Scientific, Singapore, 1994), pp. 145.

[40] T. Manago, Y. Suzuki, and E. Tamura, J. Appl. Phys. **91**, 10130 (2002).

[41] R. H. Bube, *Photoelectronic Properties of Semiconductors* (Cambridge University Press, Cambridge, 1992), pp. 244.

[42] O. M. van't Erve, R. Vlutters, P. S. Anil Kumar, S. D. Kim, F. M. Postma, R. Jansen and J. C. Lodder, Appl. Phys. Lett. **80**, 3787 (2002).

[43] We used phenomenological magneto-optical equations to estimate the spin polarization. Magneto-optical coefficients can be found in A. Berger and M. R. Pufall, Appl. Phys. Lett. **71**, 965 (1997).

[44] A. Hirohata, C. M. Guertler, W. S. Lew, Y. B. Xu, J. A. C. Bland, and S. N. Holmes, J. Appl. Phys. **91**, 7481 (2002).